JES Journal of Electrical Systems

Traveling Wave Ultrasonic Motor Type Daimler-Benz AWM90–X: Modeling and Simulation Mechanical Characteristics

F.Zohra Kebbab, Z.Boumous, S.Belkhiat

Abstract -- **During the last decade, many modeling methods, concerning TWUM, have been proposed to optimize their operational performance such as output speed, torque, power, and efficiency. In this work an analytical modeling is proposed and detailed. The study deals the mathematical model of all parts constituting the piezoelectric motor. The mechanical characteristics are deduced and presented by simulation the mathematical model under environment MATLAB / SIMULINk. . The simulation results of dynamic behavior of the motor are compared with experimental measures found in the literature, made on traveling wave piezoelectric motor standard AWM 90-X Daimler-Benz.**

Index Terms-- **Piezoelectric Motor, Analytical Modeling, Mechanical Characteristics.**

I. INTRODUCTION

Rotary ultrasonic motors have been investigated for several years. Their key features are high thrust forces related to their volume, a high holding torque without supply, high torque at low speed and good position-accuracy.

In the last two decades, a considerable progress has been achieved in the development of traveling wave ultrasonic motors (TWUM). Several works describing a range of constructions and their performance have been published [1], [2], [3]. The motors consist of a stator that uses piezoelectric elements to excite vibrations with a frequency in the ultrasonic range and a rotor (rotary motors) or a slider (linear motors) that is driven by a stator via frictional force. Depending on the geometry of the stator, generally two orthogonal vibrations (e.g., two bending vibrations) are superimposed on an elliptical motion on the contact surface between the stator and the rotor. The high-frequency and small-amplitude vibrations then are converted by friction force into a lower frequency macroscopic rotation of the rotor or a linear motion of the slider.

The operational performance of the motor (e.g., out put speed, torque, power, and efficiency) are determined mainly by the contact layer material and the prestressing force applied on the rotor. To design a TWUM, it would be valuable to have a mathematical model of the motor that takes account the contact interface, guide a proper choice of contact layer material and understand the contact layer material on motor performance. Furthermore, it would be useful for a priori calculation of motor characteristics, such as no-load speed, stall torque, maximum permissible compressive force, starting up voltage, input power, output power, and efficiency.

During the last decade, many modeling methods have been proposed for TWUM such as the equivalent electric circuit method [4], [5], and the finite element method [6], [7]. The finite element method (FEM) has been developed and extended for the vibrational analysis of piezoelectric structures [6], the steady-state performance and the analysis of a transient response applied to TWUM [7],[8]. A detailed finite element (FE) analysis of the contact surface was presented in [9], but the interaction between the interface forces and the vibrations of the stator was not considered. However, experimental techniques [10] are interesting methods for the determination of the motor characteristics but these ones cannot easily and effectively be used during preliminary design. Many analytical models of TWUM have been published in the literature [11]. Most early literature divided the modeling of TWUM into two steps. Using either analytical methods [11] or FEM [6], [8], another modeling method which integrates equivalent electric circuit, FEM, and mathematical modeling, was developed in [12]. Although the finite element modeling method provides the possibility of precise study on different mechanical parts of the motor, the complexity of FEM models make them improper for practical integration in the overall motor model [4]. It is not suitable for parameters analysis and optimization design of system [13].

In this paper, a contact-layer analysis and a mathematical model of the TWUM is presented. The analysis of contact layer is based on the consideration of contact-layer deformation, strain, and stress within it. The used model permits to run the system model on a PC with efficiency, a short simulation time and a reduced space memory. A mathematical model proposed starts from the model previously studied by Gengore [14].

In the section one a mathematical description of all components of the model is developed. The simulation of the mechanical performance under MATLAB / SIMULINK environment is presented in the section two. The theoretical simulation study are validating by comparison between the experimental results of Daimler–Benz AWM90 Motor.

F. Zohra Kebbab, Z.Boumous, S.Belkhiat are with Electrotechnic Department, DAC HR Laboratory, Ferhat Abbas University, Setif, Algeria(e-mail: Fatima_kebbab@yahoo.fr, zsid3@yahoo.fr, belsa_set@yahoo.fr

Paper presented at the Third International Conference on Electrical Engineering-ICEE'09
19-21 May 2009, USTHB, Algiers, Algeria and selected for publication in "JES" by the ICEE 2009 Editorial Board

II. MATHEMATICAL MODEL OF THE TRAVELING WAVE ULTRASONIC MOTOR

A. Basic assumptions

The structure and driving mechanism of TWUSM are special. Those include lots of non-linear and uncertain factors, and the whole drive course is very complicated.

In order to simplify model, following assumptions are made [13]:

- The rotor is rigid body, its surface is smooth;
- the friction material is visco-elastic, its surface is smooth, neglect the influence of surface roughness;
- the surface of stator teeth is continuous sinusoidal wave, neglect the influence of tooth space;
- Coulomb friction law is valid on the contact interface between stator and rotor.
- The friction layer is divided into tangential and normal system independently, which do not influence each other.

B. Model structure of the traveling wave ultrasonic motor

The objective was to build a complete model of a traveling wave ultrasonic motor using the MATLAB-SIMULINK environment. The model of the motor is structured as illustrated in Fig. 1.

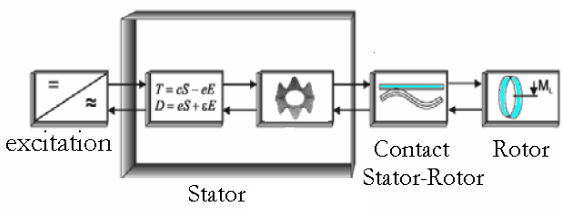

Fig.1 Functional diagram of the travelling wave ultrasonic motor

C. Dynamics of the stator deformation

To model the dynamics of the two deformation modes, we referred to the equivalent mechanical diagram of the stator shown in Fig.2.

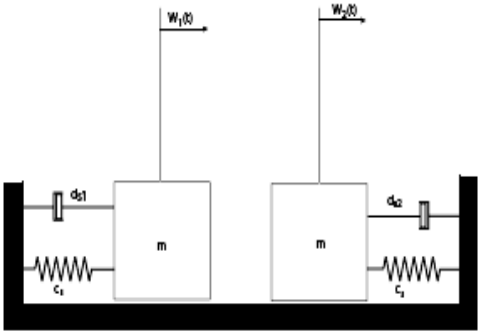

Fig. 2 Equivalent mechanical diagram of the stator dynamics deformation

This enables us to establish (1) and (2) describing the dynamics of the two stator standing waves, we obtain:

$$m_{eff}\ddot{w}_1 + d_{s1}\dot{w}_1 + c_{s1}w_1 = A_1 * \left[(1-\varepsilon_1)U_{p1} + \varepsilon_2 U_{p2}\right] + F_{s1} \quad (1)$$

$$m_{eff}\ddot{w}_2 + d_{s2}\dot{w}_2 + c_{s2}w_2 = A_2 * \left[(1-\varepsilon_2)U_{p2} + \varepsilon_1 U_{p1}\right] + F_{s2} \quad (2)$$

- m_{eff} Stator mass
- cs Equivalent rigidity of the stator.
- $ds1,2$ Damping
- $A1,2$ Force factor of piezoelectric ceramics.
- $w1,2$ Deformation amplitude of the two modes
- $U_{p1},p2$ Phases voltage

The superposition of the two standing waves creates the traveling wave which will be propagated in stator ring. In mathematical terms, this is expressed by (3), thus we obtain:

$$w(x',t) = w_1(t)\sin(kx') + w_2(t)\cos(kx') \quad (3)$$

Where $k = 2.\pi/\lambda$ is the wave number and λ is the wave length of the mode. The displacement of an unspecified point *Q* on the stator surface describes an elliptic trajectory according to (4) (a *is* the half-thickness of the stator).

$$w_Q(x',t) = w(x',t)\vec{u}_z - a\frac{\partial}{\partial x}w(x',t)\vec{u}_{x'} \quad (4)$$

The tangential speed of this point is obtained by deriving the horizontal component from the displacement vector $w_Q(x',t)$ compared to time. We obtain:

$$V_t(x',t) = -a\frac{d}{dt}\left(\frac{\partial}{\partial x'}w(x',t)\right) \quad (5)$$

The minus sign in the right-hand side of (5) indicates that the tangential speed of the points on the stator surface is in opposed direction compared to the propagation velocity of the traveling wave. Thus, the rotor is actuated in the opposed direction related to the wave.

The tangential speed of the points on the stator surface actuates the rotor thanks to the friction force which exists in the contact zone between stator and rotor. The contact zone will be studied in the next paragraph.

D. Modeling of mechanical contact between stator and rotor

With assumptions formulated in paragraph 1, (3) and (5), respectively describing the traveling wave and tangential speed, become:

$$w(x',t) = \hat{w}\cos(kx' - \omega t) \quad (6)$$

$$V_t(x',t) = \hat{V}_t \cos(kx' - \omega t) \quad (7)$$

Where $\omega = 2\pi f$, and *f* is the resonance frequency. The description of the mechanical contact between stator and rotor in the fixed reference frame related to the stator (*x*') is not advantageous. Indeed, this phenomenon can be assumed as static if we study it on a reference frame fixed arbitrarily on the traveling wave peak (x). Thanks to the position relation $x = x' - (\omega / k).t$, we can express (6) and (7) as following:

$$w(x) = \hat{w}\cos(kx) \quad (8)$$

$$V_t(x) = \hat{V}_t \cos(kx) \quad (9)$$

Now, these two relations (8) and (9) depend no more on the time. Fig. 3 shows the contact mechanism between stator and rotor for a peak of the traveling wave.

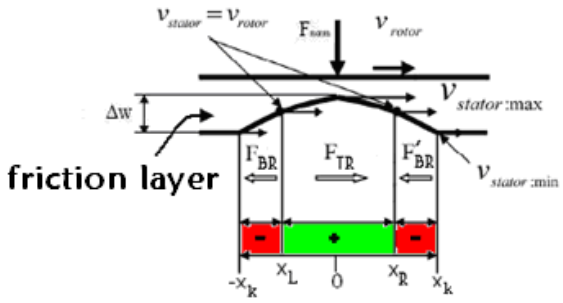

Fig .3. Diagram of the mechanical contact between stator and rotor

x_k is the width of the contact zone, x_l and x_r are the points of the stator which have the same tangential speed of the rotor. These points make it possible to locate, as shown in Fig.3, the braking and traction zones. The rotor displacement compared to the base support of the stator is noted w_R . This last will allow us, by knowing the amplitude $\hat{w}$ of the traveling wave, to determine the width *xo* of the contact zone according to (10).

$$x_k = \frac{1}{k} a\cos\left(\frac{w_R - \hat{w}}{\hat{w}}\right) \quad (10)$$

In the contact zone $(-x_0 \le x \le x_0)$, the elastic thickness contraction is given by the expression (11).

$$\Delta w = \hat{w}(\cos kx - \cos kx_k) \quad (11)$$

The vertical force per unit of length exerted in the contact zone can be expressed by (12).

$$f(x) = k_e \hat{w}(\cos kx - \cos kx_k) \quad (12)$$

ke is the equivalent rigidity of elastic thickness. The traction force per unit of length $\tau(x)$ is easily deduced from (12) by applying the law of friction. The sign function enables us to determine the braking and traction zones according to the stator/rotor contact diagram shown in Fig.3. We obtain:

$$\tau(x) = \mathrm{sgn}(V_t(x) - V_{rotor})\mu f(x) \quad (13)$$

Where μ is the dynamic coefficient of friction. The traction force can now be calculated, associated with a peak of the traveling wave, thanks to (14):

$$F = \int_{-x_k}^{x_k} \tau(x)dx \quad (14)$$

The motor torque is easily deduced from (14) knowing that in the stator ring we have *n* peak of the traveling wave.

$$T = n.R_m F \quad (15)$$

Where R_m is the average radius of the stator ring.

E. Modeling of the rotor dynamic

It is considered that the rotor has two degrees of freedom, rotation (ω_{rotor}) and vertically in the driving axis direction (w_R), as shown in the functional diagram (Fig. 2). (16) and (17) describe the rotor dynamics compared with these two degrees of freedom.

$$J\dot{\omega}_{rotor} = T - T_{load} \quad (16)$$

$$m_{rotor}\ddot{w}_R = F_Z - F_N - d_z\dot{w}_R \quad (17)$$

Where:

- J is the inertia of the rotor.
- ω_{rotor} is the rotor angular velocity of the rotor.
- T_{load} is the load torque.
- m_{rotor} is the rotor mass.
- Fz is the force exerted on the rotor in the axial direction.
- F_N *is* the force exerted by the prestressing spring.
- dz is the damping in the axial direction.

The force Fz exerted on the rotor is caused by the contraction of the elastic thickness (see Fig.3). It is given by (18).

$$F_Z = \int_{-x_k}^{x_k} f(x)dx \quad (18)$$

III. SIMULATION

Considering the parameter values of the motor [14] used for the simulation (see table-I), the mathematical model developed [15], [16], [17], [18] was simulated, in the steady and transient state of motor. The optimal parameters of the excitation voltages frequency have been tracked and evaluated to 46.65 kHz as frequency, 570 volt as excitation voltages amplitude and $\pi/2$ rd as the shift between the tow excitations .

The performances of the motor were estimated by applying various loads in the phase of the steady state after $2.5*10^{-3}$ s of operation.

The influence of the application of the loads and consequently the evolution of torque and rotor speed are presented in the following figures.

The first figure (Fig.4), described revolving rotor speed for different cases loads. The first curve represents the rotor speed without load.

From times $2.5*10^{-3}$ seconds, the motor was loaded by load torque of 1.2Nm, 2.25Nm, 3.25 Nm, 4.3Nm. It will be noticed that the speed decreases, when the applied load increases.

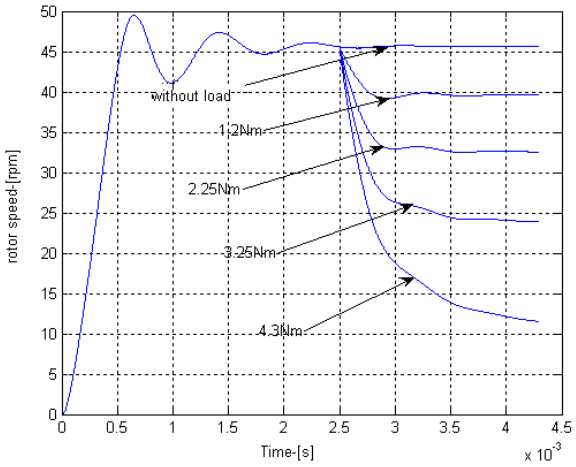

Fig. 4. Rotor-speed characteristics for various loads

The second figure (Fig.5) shows the motor torque characteristics for various loads, which illustrate what happens if a load torque is applied to the rotor after 2.5 ms of operation: the driving torque provided by the stator has to increase in order to balance the load torque. Therefore, the driving zone widens (the no-slip points move away from the wave crests), whereas the braking zones contract. The rotor velocity is equal to the stator horizontal velocity at the no-slip points; therefore, moving no-slip points down the velocity profile cause the rotor to slow down.

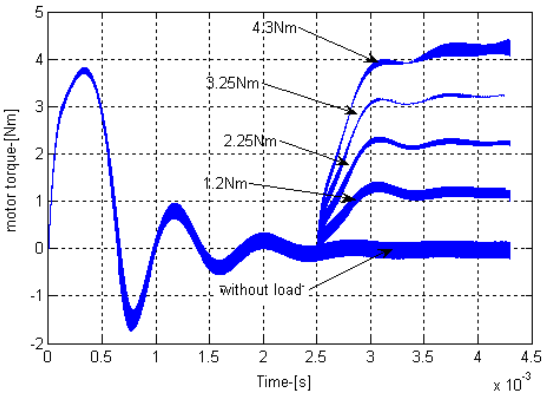

Fig. 5. Motor torque characteristics for various loads

As seen from the transient response in Fig.4, and Fig.5, the settling time of the motor is very small (≈2.5 ms). Very fast response is one of the most important advantages of the traveling wave ultrasonic motor, which makes it suitable for applications with fast response demands such as robot actuators and auto-focus cameras. Small oscillations of the rotor speed and the driving torque are caused by the no ideal traveling wave.

The Comparison of the measurements (represented by * and Δ) with the simulation results (represented by line -) are shown in Fig.6. The simulation curve overlaps with six measured values and closer to five other measured values.

The simulation results indicate that our work group implementation, on the software Matlab/Simulink, of refined model reflects the true behavior of the motor.

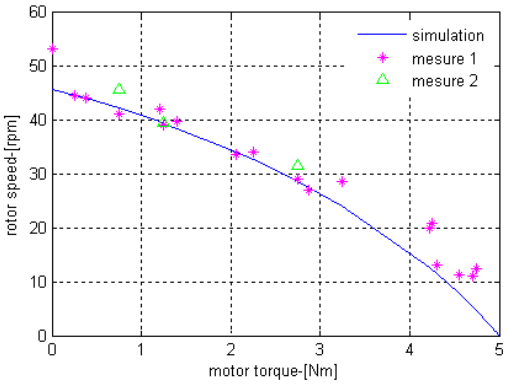

Fig.6. Measured and simulated speed-torque characteristicsof the AWM90-X motor

This shift between the measured values and the analytical curve is due to the effect of the temperature of ceramics during the friction of the stator with rotor.

IV. Conclusion

The main contribution of the work presented in this paper consists in the description of analytical modeling of traveling wave ultrasonic motor, and simulation mechanical characteristics.

As technical example of ultrasonic motor the Daimler-Benz AWM90-X motor is presented, by the measurements values obtained from the manufacturer data , and its simulation implemented by our work group.

The modeling of the traveling wave ultrasonic motor and its simulation is an important task to understand the principle of operation and its dynamic behavior.

The confirmation, the identification of simulation results and effectiveness of the mathematical model developed made by comparison with the measured results, shows that the model, reflect the real behavior of the motor, (i.e.) the model presented in this paper has the advantage to be relatively simple and quite effective.

For the new needs of applications domains, several types of piezoelectric ultrasonic motors have been suggested and designed and developed, to be used as standard as efficient, particularly the rotary traveling wave ones which are now commercially available ,and applied as auto-focus cameras, in robotics, in medical domain and in aerospace.

V. References

[1] T.Hemsel, M.Mracek, J.Twiefel, P.Vasiljev «piezoelectric linear motor concepts based on coupling of longitudinal vibrations " *ultrasonics* 44, e591-e596 ,2006.

[2] Zhijun Sun, Rentao Xing, Chunsheng Zhao, Weiqing Huang " Fuzzy auto-tuning PID control of multiple joint robot driven by ultrasonic motors " *Ultrasonics* 46 ,pp303–312, 2007 .

[3] Ikuo Yamano, Takashi Maeno " Five-fingered Robot Hand using Ultrasonic Motors and Elastic Elements " *international Conference on Robotics and Automation* ,Barcelona, Spain, April; 2005

[4] Hamed Mojallali, Rouzbeh Amini , Roozbeh Izadi- Zamanabadi, Ali A Jalali "systematic experimental based modeling of a rotary piezoelectric ultrasonic motor " *ISA transactions* 46(2007) 31-40

[5] Hirata and S. Ueha, "Design of a traveling wave type ultrasonic motor" *IEEE Trans Ultrason., Ferroelect., Freq. Contr.,* vol. 42, no. 2, pp. 225–231, 1995.

[6] Y. Kagawa and G. M. L. Gladwell, "Finite element analysis of flexure-type vibration with electrostrictive transducers" *IEEE Trans. Sonics Ultrason.*, vol. 17, no. 1, pp. 41–49, 1970.

[7] T. Yamabushi and Y. Kagawa, "Numerical simulation of a piezoelectric ultrasonic motor and its characteristics" *J. Jpn. Soc. Simul. Technol.*, vol. 8, pp. 69–76, 1989.

[8] Y. Kagawa, T. Tsuchiya, T. Yamabushi, and T. Furukawa, "Finite element simulation of dynamic responses of piezoelectric actuators" *J. Sound Vib.,* vol. 191, no. 4, pp. 519–538, 1996.

[9] T. Maeno and A. Miyaka, "Finite element analysis of the rotor/ stator contact in a ring type ultrasonic motor" *IEEE Trans. Ultrason., Ferroelect., Freq. Contr.,* vol. 39, no. 4, pp. 668–674, 1992.

[10] M. Nakamura, H. Kurebayashi, and S. Ueha, "An estimation of load characteristics of an ultrasonic motor by measuring transient response" *IEEE Trans. Ultrason., Ferroelect., Freq. Contr.*, vol. 38, no. 5, pp. 481–485, 1991.

[11] P. Hagedorn and J. Wallaschek, "Traveling wave ultrasonic motors. Part I: Working principle and mathematical modeling of the stator"*J. Sound Vib.*, vol. 155, no. 1, pp. 31–46, 1992.

[12] J. Maas, P. Ide, N. Frohleke, and H. Grotstollen, "Simulation model for ultrasonic motors powered by resonant converters" in *IEEE Industry Appl. Conf.*, 1995, pp. 111–120.

[13] Jianjun Qu , Fengyan Sun, Chunsheng Zhao "performance evaluation of traveling wave ultrasonic motor based on a model with visco-elastic friction layer on stator " *ultrasonics45*(2006) 22-31

[14] Gregor Kandare , Jorg Wallaschek "derivation and validation of a mathematical, model for traveling wave ultrasonic motors"*smart mater, struct* 11,565-574, 2002.

[15] Z.Boumous, M.Djaghloul, Z.E.Kheribeche, S.Boumous, S.Belkhiat, "Simulation of Ultrasonic Piezoelectric Motor". *International Conference on Electrical Engineering Design and Technologies ICEEDT 2*007

[16] F.Z Kebbab, Z.Boumous, S.Belkhiat ' Influence of the Prestressing Force between Stator and Rotor on the Mechanical Performance of the Travelling Wave Ultrasonic Motor Type Daimler-Benz AWM90–X'*5th International Conference on Electrical Engineering 27 - 29 October 2008 Banta (CEE 2008)*

[17] F.Z Kebbab, M. Djaghloul, Z.Boumous, S.Belkhiat 'Rotary Ultrasonic Motors: Daimler-Benz AWM 90–X TWUSM motor, Experimental and Simulation mechanical characteristics *2 nd International Conference on Electrical Engineering Design and Technologies ICEEDT'08 8-10 Novembre 2008 HAMMAMET, TUNISIA*

[18] Z.Boumous , S.Belkhiat F.Z Kebbab ' Effect of shearing deformation on the transient response of a traveling wave ultrasonic motor '*Sensors and Actuators A 150 (2009) 243–250*

Paper presented at the Third International Conference on Electrical Engineering-ICEE'09
19-21 May 2009, USTHB, Algiers, Algeria and selected for publication in "JES" by the ICEE 2009 Editorial Board

TABLE I
PARAMETERS OF AWM90-X MOTOR [14]

Name	Symbol and value
Resistances of entries	Rp_1= 5 Ω Rp_2= 5 Ω
Ceramics capacity	Cp_1= 7.8e-9 *F* Cp_2= 7.87e-9 *F*
Capacity of stator	Cp_{s1}= 0.42e-9 Cp_{s2}= 0.428e-9
Inertia of Rotor	J_R=3.4367e-004 Kgm^2
Ray	R_w = 40.5e-3 *m*
Effective mass	m_{eff} = 40.5 *Kg*
Mass of rotor	m_R = (m_{eff}+22.8+3)*1e-3 *Kg*
The rigidity of Rotor	c_R =300e3 *N/m*
Attenuation of Rotor	d_R =50*1e3 Ns/*m*
Coefficient of Coulomb of friction	μ = 0.21
The distance enters the points of surface of stator	a=4.5e-3 *m*
Peak of wave numbers	n=11
Frequency of Resonance	Wres2=wres1 wres1=2*pi*43.365*1e3 Hz
Wavelength	λ=2*pi*R_w/n *m*
Wave numbers	k=2*pi/λ
The rigidity of the zone of contacts	c_N=8500*1e6 N/m^2
Frequency of Antiresonance	w_{ant2}=w_{ant1} w_{ant1}=2*pi*46.65 e3 Hz
Modal mass of Stator	m=0.082 *Kg*
Report/ratio of transfer	A1=(m*C_{p1}*(w_{ant1})^2-w_{res1})^2))$^{1/2}$($kgFs^{-2}$)$^{1/2}$ A2=(m*C_{p2}*(w_{ant2})^2-w_{res2})^2))$^{1/2}$($kgFs^{-2}$)$^{1/2}$
Rigidity of the stator	c_{S1}=(w_{res1})^2*m *N/m* c_{S2}=(w_{res2})^2*m *N/m*
Factor of disturbance	ε1= ε2,ε1 =0.02
Damping ratios	d_{S2}=d_{S1} ,d_{S1}=10 *Ns/m*

Paper presented at the Third International Conference on Electrical Engineering-ICEE'09
19-21 May 2009, USTHB, Algiers, Algeria and selected for publication in "JES" by the ICEE 2009 Editorial Board